JOURNAL OF SPACECRAFT AND ROCKETS
Vol. 35, No. 2, March–April 1998

Engineering Notes

ENGINEERING NOTES are short manuscripts describing new developments or important results of a preliminary nature. These Notes cannot exceed 6 manuscript pages and 3 figures; a page of text may be substituted for a figure and vice versa. After informal review by the editors, they may be published within a few months of the date of receipt. Style requirements are the same as for regular contributions (see inside back cover).

Computational Dynamic Analysis of Extravehicular Activity: Large-Mass Handling

Dava J. Newman* and Grant Schaffner†
Massachusetts Institute of Technology, Cambridge, Massachusetts 02139

Introduction

COMPUTATIONAL multibody dynamics were used to simulate astronaut extravehicular activity (EVA) involving manipulation of a large-mass payload. This research effort starts to fill a current gap in quantitative analysis of EVA by solving the equations of motion, with emphasis on Kane's method. The application of dynamic simulation to EVA was prompted by the realization that physical microgravity simulators have inherent limitations: viscosity in neutral buoyancy tanks, friction in air-bearing floors, short duration for parabolic aircraft, and inertia and friction in suspension systems. A specific EVA, namely, astronaut circular trajectory manipulation of a 1201-kg payload, serves as the subject of the two dynamic simulations described herein. These simulations are modeled after an actual large-mass-handling EVA performed on Space Shuttle mission STS-63 in February 1995 when astronauts manipulated the Spartan astronomy payload as practice for future space-station EVAs.

Our contributions include a multisegment astronaut model and dynamic analysis of EVA tasks, thereby enhancing existing EVA simulations that produce either high-resolution, three-dimensional computer images based on anthropometric representations[1,2] or empirically derived predictions of astronaut strength based on lean body mass and the position and velocity of the body joints[3,4] without physics-based dynamic analysis of EVA tasks. Our physics-based methodology predicts astronaut joint positions and torques required to perform an EVA task but does not yet account for the mechanical effects of a space suit.

Methods

The astronaut model consists of seven segments with an additional eighth segment representing the large payload being manipulated. Motion was restricted to a plane of symmetry (sagittal), and the limbs on each side of the body executed identical movements. The astronaut model (Fig. 1) includes geometry and mass properties; the trunk and legs initially were set to the neutral body posture for weightlessness.[5] The astronaut's feet are considered fixed in an inertial frame called "ground" (assuming the foot restraint, Remote Manipulator System, and the Orbiter are infinitely stiff and massive).

An objective of this simulation was to specify the motion in terms of endpoint coordinates alone by specifying the position and orientation of the astronaut's hand in terms of global coordinates, similar to the way that EVA tasks are described in training, e.g., "Move the Spartan payload 1 m forward." To prescribe endpoint (hand) motion, the model incorporates a virtual planar joint between ground and the c.m. of the hand. This joint has three degrees of freedom: X displacement, Y displacement, and Z rotation. The joint position and velocity initial conditions are required for inverse kinematics and dynamics calculations.

A system description file specifies each limb segment, the name of the inboard segment, the type of joint, whether the motion of the joint is prescribed, the mass of the segment, the moments of inertia, a vector from the limb segment's c.m. to the joint axis, a vector from the inboard segment's c.m. to the joint axis, and a vector indicating the direction of the joint's axis or axes. The system description file serves as input to the dynamic equation formulation program (SD/FAST, Symbolic Dynamics, Inc., Mountain View, California) and the output is a set of functions (subroutines) in C code that implicitly represent the equations of motion of the system. The equations of motion of the multibody system are formulated as

$$M\dot{u} = \boldsymbol{F} \tag{1}$$

where M is an $n \times n$ positive-definite mass matrix, $\boldsymbol{F}$ is a $1 \times n$ force vector, and u represents Kane's generalized velocities ($\dot{u}$ denotes accelerations). Kane's method utilizes the following, highly efficient, formula for obtaining the mass matrix elements:

$$m_{rs} = \sum_{k=1}^{B} \left(m_k v_r^{k^*} \cdot v_s^{k^*} + w_r^{k^*} \cdot I_k \cdot w_s^{k^*} \right) \qquad (r, s = 1, \ldots, n) \tag{2}$$

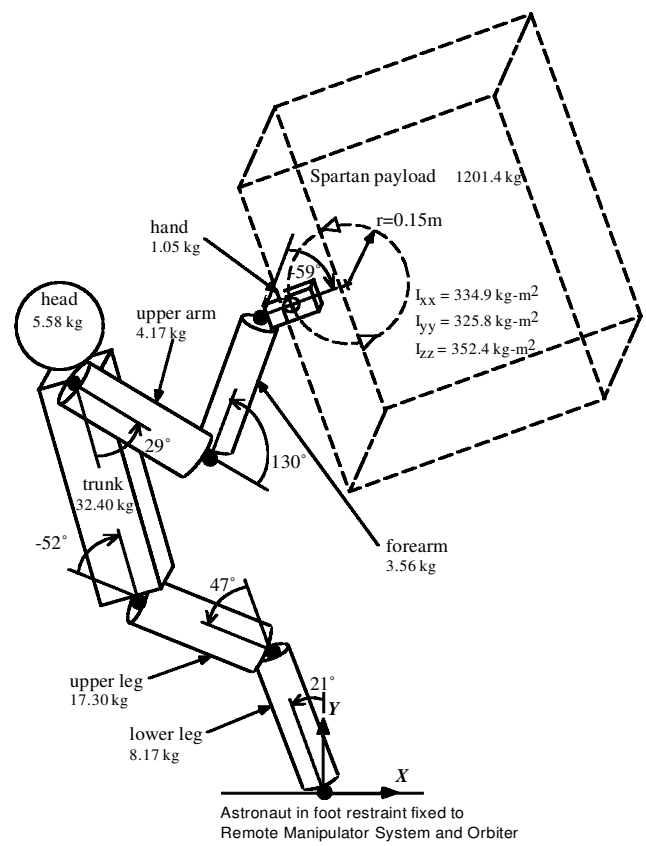

Fig. 1 Astronaut model for fixed-lower-body EVA computer simulation.

Received July 22, 1997; revision received Nov. 13, 1997; accepted for publication Nov. 17, 1997.

*Assistant Professor, Department of Aeronautics and Astronautics, Room 33-119. Member AIAA.

†Research Assistant, Department of Aeronautics and Astronautics, Room 37-219.

where m_k is the mass of the segment k, v_r^{k*} is the partial linear velocity for k, w_r^{k*} is the partial angular velocity, B is the total number of segments, and I_k is the central inertial dyadic of body k (Ref. 6).

The velocity of the endpoint segment, i.e., the c.m. of an astronaut's hand, can be calculated from the velocities of the joints of all segments by means of a Jacobian matrix J, providing the geometrical relationship between the endpoint coordinate system, referenced to an inertial frame of reference, and the joint coordinates, referenced to the inboard joint's coordinate frame, and is expressed as

$$\dot{\boldsymbol{p}} = J\dot{\boldsymbol{q}} \tag{3}$$

where $\dot{\boldsymbol{p}}$ and $\dot{\boldsymbol{q}}$ are the multibody linkage endpoint and joint velocity vectors, respectively. The positions of the endpoint and joints can be obtained by integrating these velocities over time. In contrast, joint kinematics are determined using only the endpoint kinematics, by inverting matrix (3). Employing inverse dynamics, the values of joint position, velocity, and acceleration calculated during the inverse kinematics phase are used to prescribe body joint motion rather than the planar joint connecting the hand to the ground. For each time step, the amount of torque required in each joint to bring about the prescribed kinematic system state is calculated. Animation and data plots are displayed simultaneously to correlate the numerical results with three-dimensional images.

In the initial large-mass-handling simulation, the astronaut manipulates the payload along a prescribed circular trajectory using counterclockwise arm motions [15-cm radius in 10 s, $\omega = 0.628$ rad/s (36 deg/s)], whereas the legs and trunk of the astronaut remain fixed. Using inverse kinematics, the angular position, velocity, and acceleration of the c.m. of the hand were prescribed in endpoint coordinates by

$$\theta = \pi + \omega t$$

$$\begin{cases} x_{\text{c.m.}} = x_o + r(1 + \cos\theta) \\ y_{\text{c.m.}} = y_o + r\sin\theta \end{cases} \qquad \begin{cases} \dot{x}_{\text{c.m.}} = -\omega r\sin\theta \\ \dot{y}_{\text{c.m.}} = \omega r\cos\theta \end{cases} \tag{4}$$

$$\begin{cases} \ddot{x}_{\text{c.m.}} = -\omega^2 r\cos\theta \\ \ddot{y}_{\text{c.m.}} = -\omega^2 r\sin\theta \end{cases}$$

where θ is the endpoint angular position, ω is the angular velocity, t denotes time, r is the radius, $x_{\text{c.m.}}$ and $y_{\text{c.m.}}$ are the c.m. x and y endpoint positions in global coordinates, respectively; x_o and y_o are the initial x and y positions, respectively; and the dots denote derivatives. The values for the joints were calculated using an inverted Eq. (3) at each time step.

In the second simulation the astronaut again manipulates the large payload in a circular trajectory, but realism is improved and excessive wrist motion and torque are minimized. The hip, knee, and ankle joints are allowed to move and are no longer fixed, resulting in additional degrees of freedom and a nonunique solution. We utilized a linearized least-squares root finder to determine the joint angles (and their derivatives) required for the prescribed endpoint motion and to avoid multiple solutions. Torsional springs and dampers were implemented at the hip, knee, and ankle joints to apply torques in proportion to the displacement and angular velocity of these joints. The controlled lower-body joint torques are modeled as

$$\upsilon = -K(q - q_{\text{des}}) - B\dot{q} \tag{5}$$

where υ is the passive joint torque, q is the joint angle measured from the reference position, q_{des} is the desired joint angle, $\dot{q}$ is the joint angular velocity, and K and B are the spring and damping constants, respectively. The starting configuration of the astronaut's body was enhanced by setting the wrist angle to 0 deg, the elbow to 90 deg, and the shoulder to 0 deg, i.e., alongside the trunk, placing each joint approximately halfway between its mobility limit, thus reducing the astronaut's available work envelope, so that the radius of the manipulation trajectory was reduced by half to 7.5 cm. To further reduce torque requirements, the speed of the trajectory was reduced by half to 1 revolution every 20 s.

Results

First Simulation: Fixed Lower Body

The payload manipulation is accomplished solely by the wrist, elbow, and shoulder because the lower body joints are fixed. Figure 2 shows arm joint angles (solid lines, left axis) and calculated joint torques (right axis) vs time. The results were compared to published space-suit mobility limits[5] and an astronaut-physiological-strength database.[3,4] The elbow and shoulder angles are within mobility limits, but the wrist joint significantly exceeds the negative angle limit of −28 deg, reaching as much as −68 deg (denoted by pluses). The calculated limb joint torques reveal smooth sinusoidal curves partly because of the circular manipulation trajectory and partly because the torques are distributed among the joints. The hip, knee, and ankle joints reveal the amount of torque required to fix these joints at the

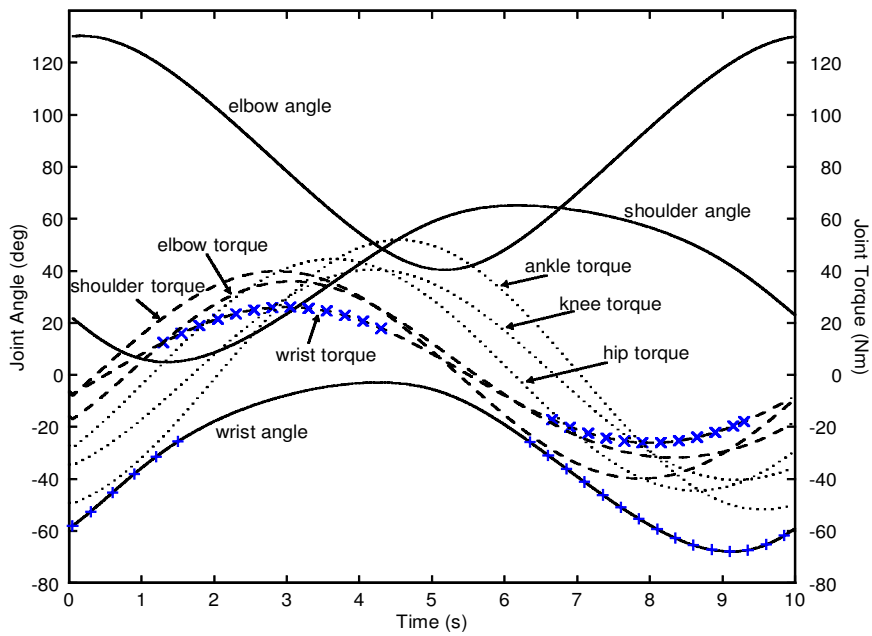

Fig. 2 Limb joint angles (——) and torques for hip, knee, and ankle (·····) and wrist, elbow, and shoulder (– – –) vs time.

Table 1 Compliant-lower-body simulation of joint angles, velocities, accelerations, and torques

	Refs. 4 and 5				Current study							
	Angle, deg		Torque, Nm		Angle, deg		Velocity, deg/s		Acceleration, deg/s^2		Torque, Nm	
Joint	Max	Min	Max	Min	Max	Min	Max	Min	Max	Min	Max	Min
Wrist	22.8	−28.3	13.1	−17.2	21.0	−9.0	5.2	−4.6	4.6	−5.2	3.3	−3.3
Elbow	130.0	0.0	45.6	−48.1	100.0	51.0	9.7	−13.2	10.3	−18.3	4.5	−4.5
Shoulder	180.0	0.0	71.2	−66.4	25.0	−5.0	8.6	−9.7	12.0	−6.9	5.0	−5.1
Hip	0.0	−70.0	——	——	−51.0	−56.0	0.6	−1.7	10.9	−2.3	5.0	−5.1
Knee	120.0	0.0	——	——	49.0	46.0	1.2	−1.2	1.7	−4.6	4.7	−4.2
Ankle	40.0	−40.0	——	——	23.0	19.0	2.3	−1.2	2.3	−1.7	6.1	−5.0

specified angle, and the ankle-joint torque reaches a maximum of 52 Nm. The elbow- and shoulder-joint torques remain within limits, but the wrist joint significantly exceeds physiological strength limits. The 26-Nm maximum calculated wrist torque is well above the 13-Nm limit, and the maximum negative torque of −26 Nm is significantly beyond the limit of −16 Nm (denoted by multiplication signs).

Second Simulation: Compliant Lower Body

Joint-angle time histories and joint torques were calculated for all six body joints, and Table 1 provides a summary of the maximum and minimum joint angles, velocities, accelerations, and torques for the compliant-lower-body simulation. The wrist and elbow angular excursions remain well within the space-suit limits, but the shoulder joint deviates slightly beyond the lower limit of 0 deg by 5 deg. The lower-body joint angles are no longer fixed and exhibit slight fluctuations in accordance with the modeled compliance. All calculated joint torques fall within physiological limits and are approximately one-eighth of their values in the first simulation.

Discussion

The seven-segment planar astronaut model and large-mass-handling task for our two dynamic simulations provide a new methodology for EVA research. The simulated motion is described in endpoint coordinates, allowing for comparisons to actual EVA training tasks. The corresponding astronaut model joint motions are calculated by inverse kinematics, yielding joint position, velocity, and acceleration. The torque required in each joint for the prescribed kinematic motion is calculated through inverse dynamics.

In the first simulation with fixed lower-body angles, the wrist joint exceeded the space-suit range of motion by 40 deg, and the torque values demanded of the wrist were twice that of human capability because of the size and speed of the trajectory and the inertial properties of the payload. The first simulation was modified so that it could be accomplished within the bounds of human capability, illustrating a primary simulation objective: to identify problems that might be masked by the limitations of physical simulators before they are encountered during an actual microgravity EVA and to assist mission designers and trainers.

The second simulation addressed these problems by starting with the arms in a more reasonable position, allowing the wrist to remain within its range of motion, and reducing the radius and speed of the manipulation trajectory by half so that the torque levels remain within limits. The realism of the first simulation is enhanced in the second by modeling the passive impedance characteristics of muscles, tendons, and ligaments in the legs via mechanical analogs, i.e., torsional springs and dampers. This results in a significant improvement over previous astronaut models, incorporating biomechanics literature[7,8] into EVA task analysis for the first time. Upon detailed inspection of the results, the astronaut's body was seen initially to tilt backward as the payload was pushed along the lower half of the circular trajectory and then to tilt forward as the payload was pulled along the upper half of the trajectory, reflecting accurate inertial modeling of the microgravity EVA large-mass-handling task. There were no available data on ankle-joint torque limits, but a value of 52 Nm is relatively large and may give analytical insight into numerous astronauts' complaints about ankle fatigue during EVA tasks. Our 1-*g* optimized human body, specifically, our small antigravity ankle musculature, is not designed to counteract the large-moment arm induced through the ankles when an astronaut is performing upper-body arm tasks during microgravity EVA while constrained in foot restraints.

Conclusions

This research demonstrates the feasibility and utility of simulating EVA tasks by means of computational methods. The advantages include the ability to obtain quantitative dynamics data of interest, i.e., joint angular excursions and torque requirements; the avoidance of the limitations of physical simulators; and the ease of running successive simulations with modifications.

Acknowledgments

This research effort was supported under NASA Grant NAGW-4336. The authors wish to thank David Rahn for all of his computer animation work in making this project a success; Robert Callaway and Bruce Webbon from NASA Ames Research Center, Mike Rouen from NASA Johnson Space Flight Center, and Ron White from NASA Headquarters for their encouragement and support; Abilash Pandya and Jim Maida from NASA Johnson Space Flight Center for providing the human-strength predictions; and Mike Sherman and Dan Rosenthal of Symbolic Dynamics for technical assistance.

References

[1] Price, L. R., Fruhwirth, M. A., and Knutson, J. G., "Computer Aided Design and Graphics Techniques for EVA Analysis," *Proceedings of the Twenty-Fourth International Conference on Environmental Systems and Fifth European Symposium on Space Environmental Control Systems* (Friedrichshafen, Germany), Society of Automotive Engineers, Warrendale, PA, 1994, pp. 1–13.

[2] "The McDonnell Douglas Human Modeling System MDHMS," Ver. 2.2, McDonnell Douglas Aerospace-West, McDonnell Douglas Corp., MDC-93K0283, Long Beach, CA, Sept. 1993.

[3] Pandya, A. K., Hasson, S. M., Aldridge, A. M., Maida, J. C., and Woolford, B. J., "Correlation and Prediction of Dynamic Human Isolated Joint Strength from Lean Body Mass," NASA TD-3207, 1992.

[4] Morgan, D., Wilmington, R., Pandya, A. K., Maida, J., and Demel, K. J., "Comparison of Extravehicular Mobility Unit (EMU) and Unsuited Isolated Joint Strength Measurements," NASA TD-3613, 1996, pp. 1–46.

[5] "Man-Systems Integration Standards," NASA STD-3000, Vol. 1, Rev. 1, 1995, pp. 14-1–14-65.

[6] Rosenthal, D. E., and Sherman, M. A., "High Performance Multibody Simulations via Symbolic Equation Manipulation and Kane's Method," *Journal of the Astronautical Sciences*, Vol. 34, No. 3, 1986, pp. 223–239.

[7] McMahon, T. A., "Mechanics of Locomotion," *International Journal of Robotics Research*, Vol. 3, No. 2, 1984, pp. 4–27.

[8] Hogan, N., "Impedance Control: An Approach to Manipulation, Part 1: Theory," *Journal of Dynamic Systems, Measurement and Control*, Vol. 107, March 1985, pp. 1–7.

R. B. Malla
Associate Editor